Localization of an RF source inside the Human body for Wireless Capsule Endoscopy

Rohit Chandra
rohit.chandra@eit.lth.se

Anders J Johansson
anders.j.johansson@eit.lth.se

Fredrik Tufvesson
fredrik.tufvesson@eit.lth.se

Dept. of Electrical and Information Technology
Lund University, Box 118, SE-22100, Lund, Sweden

ABSTRACT

This paper presents a method based on the phase difference of arrival and the non-linear least square estimation to localize a radio-frequency (RF) source, e.g a wireless capsule endoscope, inside the human body. The phase difference of arrival at multiple frequencies of a signal is used to estimate the distance of the source to a receiver. The linear least square estimation is used to estimate the initial position of the source followed by a non-linear least square method to improve the localization accuracy. The method is applied on noise free simulated data obtained from FDTD simulations in the 403.5 MHz MedRadio band of a simple homogeneous phantom and a more realistic heterogeneous phantom. The distance between the true position and the estimated position is found to be within 1 cm for the simulated cases showing the possibility to use the proposed method for localization of an RF source inside the human body, as long as the signal to noise ratio is high enough.

Keywords

Wireless capsule endoscopy, RF localization, phase difference, least squares

1. INTRODUCTION

Today there is an increased use of wireless technology for medical diagnosis. Wireless capsule endoscopy is one such example for diagnosing gastrointestinal (GI) tract diseases. Conventional wired endoscopy is done by inserting a long flexible tube through the mouth or the rectum, usually containing optical fibers to transmit light to illuminate the organ under inspection and capture images with a lens and a miniature camera [1],[2]. However this procedure may cause pain and discomfort. Moreover, due to the complex anatomy of the small intestine, the conventional wired endoscopy is incapable of reaching the entire small intestine [2].

The limitations of the conventional wired endoscopy can be overcome by the use of a wireless capsule endoscope (WCE) [1], [2]. A WCE is an ingestible pill-like wireless device containing a miniature camera that captures the images while it passes through the small intestine or other part of the GI tract. The images are usually sent wirelessly to an external receiver for analysis. However, one of the challenges in wireless endoscopy is accurate localization of the capsule while it passes through the GI tract due to the lossy and heterogeneous nature of the tissues of the human body. The localization is critical in order to be able to know the location from where the images are captured. If the captured image shows abnormality in the GI tract, with the knowledge of the location of the captured image, therapeutic operations could be performed precisely at the position of the abnormality.

The methods used for localization of the capsule endoscopes are usually based on the measurement of the magnetic or the electromagnetic (EM) field as discussed in [2]. The main advantage of localization methods based on the magnetic field strength is that low frequency magnetic fields can pass through the body with low attenuation as tissues of the human body are non-magnetic. However, one challenge is the interference from the magnetic fields produced by material present in the surrounding and also from the earth's magnetic field and this may require additional equipment for analysis of the magnetic signal for the localization. On the other hand, an advantage of the electromagnetic system is re-using the EM signal radiated by the WCE without any additional equipment. On the downside, high frequency EM waves have much higher attenuation as compared to magnetic waves when they pass through human tissues. Low frequency EM waves have low precision of localization.

The conventional method of localization using radio frequency signals for indoor and outdoor environments are based on received signal strength, angle of arrival (AOA), time of arrival and, time difference of arrival. AOA methods are problematic due to the multipath components arising because of the complex environment inside the human body which includes several layers of heterogeneous lossy tissues each having different electrical properties. On the other hand, time-based methods need strict time synchronization and high bandwidth for desired precision, which is hard to achieve in the MedRadio band (401-406 MHz). It could be used for ultra-wideband (UWB) based localization [3]. Hence, field strength methods based on the received signal strength indicator (RSSI) have been discussed in detail in the literature [5]-[12].

BODYNETS 2013, September 30-October 02, Boston, United States

DOI 10.4108/icst.bodynets.2013.253713

RSSI based methods use the received signal at different positions on the abdomen for localization of the capsule [6], [7]. Usually, a signal propagation model is used which relates the received signal strength with the distance between the in-body transmitter and the receiver located on the body. After the distances from the receiver are estimated, a trilateration method could be employed to calculate the coordinates of the capsule. In [8], instead of using a propagation model, the authors used an algorithm based on a lookup table where offline measurement was carried for different positions of the WCE and stored in a look up table. Later on during the experiment, the RSSI was compared with the closest value in the look up table for position estimation. There has been efforts to build a more accurate propagation model which does not only depend upon the distance but also the antenna orientation and tissue absorption [9], [10]. Thus, the RSSI based methods need a propagation model which varies from person to person due to complex radio wave absorption properties of the human tissue [2].

There are also radio frequency identification (RFID) based methods of localization investigated in [13]-[17] that in some way or the other rely on the field strength measurements. In [13], a cubic antenna array is built around the patient's body to track the RFID tag integrated in the WCE. The localization algorithm is based on the assumption that the closest antenna detects the tag. An improved method consisting of RFID tags having bi-directional antennas are discussed in [14], [15]. Phase difference of the signal from an RFID tag without any localization algorithm is discussed in [16]. Using this approach, the authors in [17] use support vector regression to track the medical instruments such as needles and catheters having RFID tag with a mean accuracy in the mm range. However, the tags orientations were kept fixed and the influence of the human tissues on the RF signal was not considered.

With the exception of AOA based methods, the first step for the localization methods is the estimation of the distance (also called ranging) from the transmitter to the different receivers. Hence, a more accurate distance estimate will result in a more accurate position estimate. The main contribution of this paper is to develop a ranging method based on the phase difference of the electromagnetic signal for different frequencies received at the same receiver antenna for a case when the transmitter is implanted and the receivers are located on the body. The phase difference method has been used for the localization in a free space [16] and can be seen as a variant of time of arrival based methods. In this paper, we develop a formulation to extend it for the implant to the on-body case. A linear least square method is used to get an initial position estimate of the RF source using the estimated distance from different receivers as discussed for free space localization in [19]. This initial estimate of the location is then used as an input for the non-linear least square model for localization which is an iterative method for more accurate localization. A similar approach using the non-linear least square method, however, based on the RSSI for the range estimation at the 433 MHz band is discussed in [6], [11].

The method developed in this paper is applied on simulated data obtained through FDTD simulations done with a simple cylindrical homogeneous phantom, and with a more realistic heterogeneous phantom, in the 403.5 MHz MedRadio band. The localization is done for 2D case with the capsule inside the homogeneous and the heterogeneous phantom. It is then extended to a 3D case for the homogeneous phantom.

The data from the capsule is transmitted to the on-body sensors connected to a data recorder worn with a belt. The frequency of the data transmission is usually twice per second as in Given Imaging endoscopy capsules [20]. It should be noted that the proposed localization method is a supplement to such a WCE system where the recorded data is used in a post processing step for the localization of the capsule. Hence, the computational complexity of the proposed algorithm is not considered, which can be critical for the real time tracking systems.

2. LOCALIZATION ALGORITHM

The localization system assumes that there are N receive antennas placed on the body at known positions around the abdomen such that $N \geq 3$ for 2-D localization and $N \geq 4$ for 3-D localization. These N receive antennas receive the signal from the capsule after it has traveled through the lossy tissues having effective relative permittivity ϵ_r and effective conductivity σ. More details about the electrical properties of the medium are given in Section 5. The presented localization method is a three step process. In the first part of the localization algorithm, the distance of the receiver from the capsule is estimated. Using this estimated distance, in the second step, initial coordinates of the capsule are obtained using a linear least square method. This initial estimate of the coordinates is then used in the final step based on the non-linear least square method for the estimation of more accurate coordinates of the capsule. The details of each step are described below.

2.1 Estimation of the distance

The phase ϕ_i of the signal received at the ith receiver is given by

$$\phi_i = \phi_{ki} + \phi_{di}, \tag{1}$$

where ϕ_{ki} is the phase offset between the transmitter and the ith receiver, which is assumed to be constant, and $\phi_{di} = -\beta d_i$ is the phase of the signal after traveling through a distance d_i in the medium with phase constant β and effective relative permittivity ϵ_r and effective conductivity σ. The phase constant at frequency f of the medium is given by [21]

$$\beta = 2\pi f \sqrt{\frac{\mu_0 \epsilon_0 \epsilon_r}{2} \left(\sqrt{1 + \left(\frac{\sigma}{2\pi f \epsilon_0 \epsilon_r} \right)^2} + 1 \right)}, \tag{2}$$

where μ_0 is the permeability and ϵ_0 is the permittivity in free space. Substituting $\phi_{di} = -\beta d_i$ in (1) and differentiating w.r.t. frequency f, the first term ϕ_{ki} being a constant will vanish and we get

$$\frac{\mathrm{d}\phi_i}{\mathrm{d}f} = -d_i \frac{\mathrm{d}\beta}{\mathrm{d}f}. \tag{3}$$

Differentiating β w.r.t to frequency, the estimated distance $\hat{d}_i$ is given by

$$\hat{d}_i = -\frac{c}{\sqrt{2}\pi K\sqrt{\epsilon_r}}\frac{\mathrm{d}\phi_i}{\mathrm{d}f}, \tag{4}$$

where d_i is approximated by the estimated distance $\hat{d}_i$, $c = 1/\sqrt{\mu_0\epsilon_0}$ is the speed of light in vacuum, and K depends upon a factor $P = 1 + \left(\frac{\sigma}{2\pi f\epsilon_0\epsilon_r}\right)^2$ and is given by

$$K = \sqrt{\sqrt{P}+1} - \frac{P-1}{2\sqrt{P(\sqrt{P}+1)}}. \tag{5}$$

From (4), it can be seen that the estimated distance depends upon the slope of the phase of the received signal in the frequency domain.

2.2 Estimation of the initial estimate of the coordinates

We use the method described in [19] for free space and extended it to the WCE case in [6] for the estimation of the location. Let $\Omega = (x, y, z)$ be the coordinates of the capsule at a time instant t. The position of the ith receiver is given by $R_i = (x_i, y_i, z_i)$. The true distance between the ith position R_i and the capsule location Ω is given by $d_i(\Omega) = \sqrt{(x-x_i)^2 + (y-y_i)^2 + (z-z_i)^2}$. In this method, one of the receivers is assumed to be reference. Let the coordinates of this reference receiver be $R_r = (x_r, y_r, z_r)$. The true distance between the reference receiver and any receiver is given by $d_{ir} = \sqrt{(x_i-x_r)^2 + (y_i-y_r)^2 + (z_i-z_r)^2}$. Similarly, the true distance between the capsule location and the reference receiver is given by: $d_r(\Omega) = \sqrt{(x-x_r)^2 + (y-y_r)^2 + (z-z_r)^2}$. Using the cosine rule, we can derive the following equation:

$$(x_i-x_r)(x-x_r) + (y_i-y_r)(y-y_r) + (z_i-z_r)(z-z_r) = \frac{1}{2}(d_r(\Omega)^2 + d_{ir}^2 - d_i(\Omega)^2). \tag{6}$$

Since, the coordinates of the receiving antennas are known, d_{ir} is a known quantity. $d_r(\Omega)$ can be replaced by the estimated distance $\hat{d}_r(\Omega)$ and $d_i(\Omega)$ by $\hat{d}_i(\Omega)$ in (6). Assuming the nth receiver, $R_n = (x_n, y_n, z_n)$ to be a reference receiver, we will get a linear system with $N-1$ equations in 3 unknowns x, y and z. The equations can be written in matrix form as

$$\mathbf{Ax} = \mathbf{b}, \tag{7}$$

where $\mathbf{A}$ is given by

$$\mathbf{A} = \begin{pmatrix} x_1 - x_n & y_1 - y_n & z_1 - z_n \\ x_2 - x_n & y_2 - y_n & z_2 - z_n \\ \vdots & \vdots & \vdots \\ x_N - x_n & y_N - y_n & z_N - z_n \end{pmatrix}, \tag{8}$$

and here the n^{th} row having zero elements has been omitted. Finally, $\mathbf{x}$ is given by

$$\mathbf{x} = \begin{pmatrix} x - x_n \\ y - y_n \\ z - z_n \end{pmatrix} \tag{9}$$

and $\mathbf{b}$ is given by

$$\mathbf{b} = \begin{pmatrix} 0.5(\hat{d_n}(\Omega)^2 + d_{1n}^2 - \hat{d_1}(\Omega)^2) \\ 0.5(\hat{d_n}(\Omega)^2 + d_{2n}^2 - \hat{d_2}(\Omega)^2) \\ \vdots \\ 0.5(\hat{d_n}(\Omega)^2 + d_{Nn}^2 - \hat{d_N}(\Omega)^2) \end{pmatrix}. \tag{10}$$

The solution of (7) is given by

$$\mathbf{x} = (\mathbf{A^T A})^{-1}\mathbf{A^T b} \tag{11}$$

where $(.)^{\mathrm{T}}$ represents the transpose of a matrix. In cases where $\mathbf{A^T A}$ is nearly singular and poorly conditioned, its inverse cannot be calculated. For such cases, the solution can be calculated by back substitution after doing $\mathbf{QR}$ decomposition of the matrix $\mathbf{A}$ [19].

2.3 Estimation of the coordinates by Non-Linear Least Square method

The initial estimates calculated in Section 2.2 is used as the input for calculating the final estimate of the capsule location by the non-linear least square method [19]. The non-linear least square method is a well known method for error minimization and is described here for completeness. It minimizes the sum of the squares of the error on the exact distance $d_i(\Omega) = \sqrt{(x-x_i)^2 + (y-y_i)^2 + (z-z_i)^2}$ and the estimated distance $\hat{d}_i(\Omega)$ for all the receivers. The sum of the errors $E(\Omega)$ of the distances is given by

$$E(\Omega) = \sum_{i=1}^{i=N} (f_i(\Omega))^2 = \sum_{i=1}^{i=N} (d_i(\Omega) - \hat{d}_i(\Omega))^2. \tag{12}$$

To minimize the sum of the errors on the distances, the partial derivate of $E(\Omega)$ w.r.t. x, y and z has to equated to zero simultaneously, i.e.

$$\nabla E(\Omega) = \begin{pmatrix} \frac{\partial E(\Omega)}{\partial x} \\ \frac{\partial E(\Omega)}{\partial y} \\ \frac{\partial E(\Omega)}{\partial z} \end{pmatrix} = 0. \tag{13}$$

Equation (13) can be reduced to the following form:

$$\nabla E(\Omega) = 2\mathbf{J}(\Omega)^T\mathbf{f}(\Omega) = 0 \tag{14}$$

where $\mathbf{J}(\Omega)$ is the Jacobian defined by

$$\mathbf{J}(\Omega) = \begin{pmatrix} \frac{\partial d_1(\Omega)}{\partial x} & \frac{\partial d_1(\Omega)}{\partial y} & \frac{\partial d_1(\Omega)}{\partial z} \\ \frac{\partial d_2(\Omega)}{\partial x} & \frac{\partial d_2(\Omega)}{\partial y} & \frac{\partial d_2(\Omega)}{\partial z} \\ \vdots & \vdots & \vdots \\ \frac{\partial d_N(\Omega)}{\partial x} & \frac{\partial d_N(\Omega)}{\partial y} & \frac{\partial d_N(\Omega)}{\partial z} \end{pmatrix} \tag{15}$$

and $\mathbf{f}(\Omega)$ is a vector containing the difference of the distances $f_i(\Omega) = d_i(\Omega) - \hat{d}_i(\Omega)$ given by

$$\mathbf{f}(\Omega) = \begin{pmatrix} f_1(\Omega) \\ f_2(\Omega) \\ \vdots \\ f_N(\Omega) \end{pmatrix}. \quad (16)$$

Equation (14) can be solved by iterative methods like Newton-Raphson:

$$\Omega_{k+1} = \Omega_k - \left[\mathbf{J}(\Omega_k)^T \mathbf{J}(\Omega_k)\right]^{-1} \mathbf{J}(\Omega_k)^T \mathbf{f}(\Omega_k), \quad (17)$$

where Ω_k is a vector containing coordinates of the WCE at the kth iteration. Ω_1 is the vector of initial coordinates estimated in Section 2.2. Iterations are performed until $|\Omega_{k+1} - \Omega_k| < \xi$ such that ξ has a small value. We choose $\xi = (0.01 \quad 0.01 \quad 0.01)^T$ mm.

2.4 Performance evaluation of localization

The performance of the algorithm is evaluated by calculating the error distance (d_{err}) of the position estimate which is the distance between the true position and the estimated position and is defined as:

$$d_{err} = \sqrt{(x - \hat{x})^2 + (y - \hat{y})^2 + (z - \hat{z})^2}, \quad (18)$$

where (x, y, z) is the true position of the capsule and $(\hat{x}, \hat{y}, \hat{z})$ are the final estimated coordinates.

3. SIMULATION SETUP

The developed algorithm for the localization is tested on data obtained through finite-difference-time-domain (FDTD) simulations done with a simple homogeneous cylindrical phantom and a heterogeneous phantom from the Virtual Classroom Project [22]. Simulations are done in a commercial FDTD full-wave electromagnetic solver SEMCAD-X [23] in the 403.5 MHz MedRadio Band. The cylindrical phantom has a diameter of 10 cm and height of 10 cm, and homogeneous electrical properties ($\epsilon_r = 57.1$ and $\sigma = 0.8$ S/m) of muscle tissue at 403.5 MHz is assigned. The heterogeneous phantom used is a truncated torso part of Billie phantom [22]. For the heterogeneous phantom, the electrical properties of all the tissues are assigned at 403.5 MHz. For a preliminary investigation, a broadband simulation is done in the 401-406 MHz band and then the phase of the simulated forward transmission coefficient (S_{21}) is extracted at 5001 frequency points. The factor P, used in (5), is calculated at 403.5 MHz. The simulation domain is terminated by an uni-anisotropic perfectly matched layer (UMPL) at the boundary. A hertzian dipole of length 1 cm is used as the transmitter and the receiver. The antenna placement along with the position estimation is described in the following section.

4. POSITION ESTIMATION

In this section we describe the different cases for which the localization algorithm is implemented. The position of the feed point of the hertzian dipole is taken as the position of the receive antenna and the transmit antenna in the algorithm.

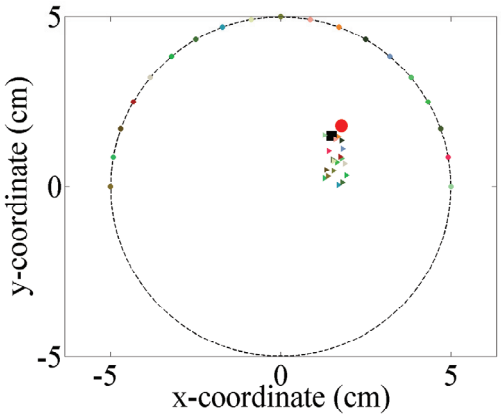

Figure 1: 2D Localization of the capsule in a cylindrical homogeneous phantom. The circle represents the cross-section of the cylindrical phantom with a diameter of 10 cm. The dots at the boundary represent the receiving antennas and the triangles shows the different initial estimates when using different receivers as a reference in the same color. The actual position of the transmitter is shown with a square at (1.5, 1.5, 0) cm. The estimated position of the transmitter is shown with a red dot at (1.79, 1.79, 0) cm.

4.1 Cylindrical Phantom: 2D case

For the cylindrical phantom in 2D, 19 receive antennas are placed along the curvature at an equal angular position of 10° at the half height of the cylinder where z = 0. The center of the cylinder is at origin O = (0, 0, 0) cm. The transmitter is at the coordinate $\Omega = (1.5, 1.5, 0)$ cm. The transmit antenna and the receive antennas have the same polarization and their axes are parallel to the axis of the cylinder. Homogeneous electrical properties of the muscle is assigned to the cylinder ($\epsilon_r = 57.1$ and $\sigma = 0.8$ S/m), and the same value is used in the algorithm. The phase of S_{21} for each receiver is extracted and the mean value of the slope $\mathrm{d}\phi_i/\mathrm{d}f$ is calculated. Each one of the receivers is chosen as a reference at one time and an initial estimate of the coordinates of the transmitter are calculated. For different reference receivers, different transmit antenna coordinates are found as shown in Fig. 1. Using the initial estimate, the final coordinate is calculated by the non-linear least square method. The solution for all the initial estimated coordinates converges at a same location having coordinates (1.79, 1.79, 0) cm. Thus, the distance error d_{err} of the position estimation is 0.41 cm. It took 5 iterations to converge at the final solution.

4.2 Heterogeneous Phantom: 2D case

The algorithm is applied on the simulated data for the heterogeneous phantom Billie from virtual classroom project [22]. Three receive antennas are placed at (-2.31, 5.59, 0) cm, (-4.06, 0.85, 0) and (-3.80, -6.09, 0) cm on the body. The transmitter is implanted at the level of the small intestine of the phantom at (1, -0.8, 0) cm with same polarization as the receiver which is parallel to the body axis (z-axis). The receive antenna positions and the transmit antenna position are shown in Fig. 2. For the estimation algorithm, the elec-

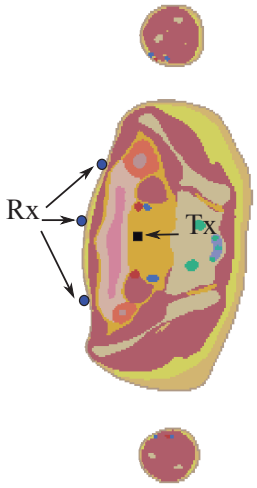

Figure 2: Example of receiver and transmitter positions shown when using the heterogeneous Billie phantom [22].

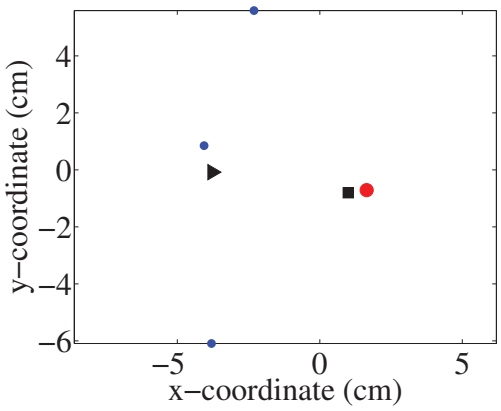

Figure 3: 2D Localization of the capsule in a realistic heterogeneous phantom. The blue dots are the receivers. The initial estimate is shown with a black triangle. The actual position of the transmitter is shown with a square at (1, -0.8, 0) cm. The final estimated position of the transmitter is shown with a red dot at (1.65, -0.71, 0) cm.

trical properties of the muscle at 403.5 MHz are used. The error in estimated distance $\hat{d}$ calculated from (4) for the three receivers is 0.7 cm, 0.07 cm, and 0.9 cm, respectively. The initial estimate of the location is at (-3.77 , -0.08, 0) cm for all the three receivers as the reference. The final estimate using the non-linear least square method is at (1.65, -0.71, 0) cm. The convergence was achieved in 6 iterations. An error of 0.65 cm is obtained in the x-coordinate and 0.09 cm in the y-coordinate which accounts to d_{err} of 0.65 cm. The localization result is shown in Fig. 3.

4.3 Cylindrical Phantom: 3D case

For the cylinder in the 3D case, four receivers are placed along the surface of the cylinder. The position of the receive antennas are randomly chosen at the positions having the coordinates (2.46, 4.45, 5.01) cm, (-3.54, 3.69, 5.51) cm, (-3.04, 4.09, 10.02) cm, and (3.06, 4.05, 9.51) cm. The transmit antenna is placed at (0, 3, 7.51) cm. The polarization of all the antennas is the same and parallel to the axis of the cylinder. The error in estimated distance $\hat{d}$ calculated from (4) for the four receivers is 0.03 cm, 0.36 cm, 0.04 cm, and 0.45 cm, respectively. For all the receivers as the reference, the initial estimated position of the transmitter is found to be the same at (0.26, -0.80, 7.47) cm. It can be seen that the accuracy of the initial estimate is poor. However, using this initial estimate with the non-linear least square algorithm, the final estimate is found to be at (0.017, 3.54, 7.54) cm. It took 677 iterations for Newton-Raphson to converge at the final solution. d_{err} of the estimated position is 0.54 cm. The result of the position estimation for 3D case is shown in Fig. 4.

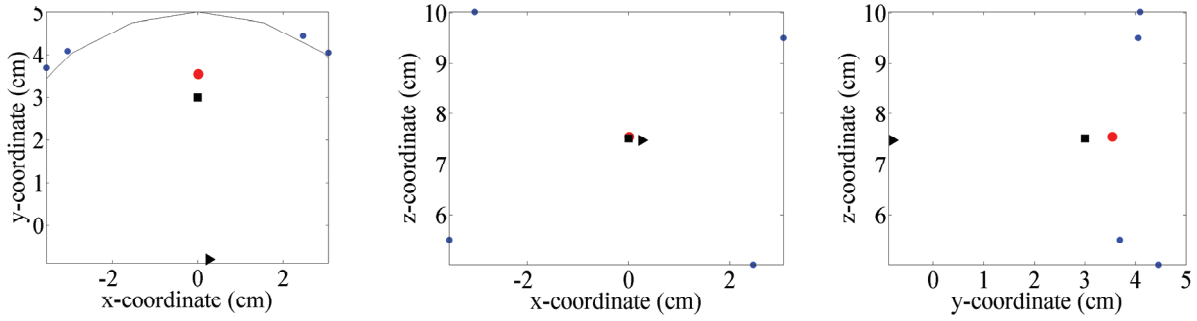

(a) (b) (c)

Figure 4: 3D localization of the WCE in a homogeneous cylindrical phantom. The actual position of the WCE, (0, 3, 7.51) cm, is shown with a black square whereas the final estimated position at (0.017, 3.54, 7.54) cm, is shown with a red dot. The black triangle shows the position of the initial estimate and the receivers are shown with blue dots. (a) Position estimate in the x-y plane. Part of the phantom boundary is also shown. (b) Position estimate in the x-z plane (c) Position estimate in the y-z plane.

5. DISCUSSIONS AND FUTURE WORK

The proposed localization method developed in the paper is for a WCE system where the data is analyzed in a post processing step. It should be noted that since the algorithm for localization would be used during post processing and not in a real time, the computational complexity of the algorithm is not a direct limitation.

The set of the coordinates used in the localization is taken from an absolute coordinate system. In a practical application, the coordinate system can be defined w.r.t. to the position of one of the receive antennas. There might be some additional error in the position estimate due to breathing, which will alter the coordinate system

One of the requirements of the algorithm is that the electrical properties (relative permittivity and conductivity) of the tissues should be known. We used the homogeneous electrical properties of muscle tissue on the simulated data from the heterogeneous phantom. For more accurate localization, the proper effective electrical properties of the tissues have to be estimated and used. The method described in [18], where the effective electrical properties are estimated using a magnetic resonance imaging scan (MRI) of the body, could be used. The drawback is that it requires a costly MRI scan of the patient. Other methods for determination of the proper effective electrical properties will be investigated in the future.

In the current analysis, noise is ignored. In practical scenarios noise will be present and will influence the localization result. Another limitation in the current analysis is the polarization of the antennas. All the receive antennas and the transmit antenna are linearly polarized in the same direction. However, in reality the capsule will change orientation while traveling through the GI tract and hence there might be polarization miss-match resulting in poor signal-to-noise ratio. One solution to this is an antenna system that uses polarization diversity either at the receiver or transmitter side.

The dependency on the number of antennas for the localization will also be investigated. Another field to investigate is localization in the 3D heterogeneous case. In this paper, the algorithm is tested on a few examples and hence more simulations with different positions of the transmitter and the receiver would be done to arrive at a statistical conclusion regarding the performance of the algorithm.

6. CONCLUSIONS

A method based on phase difference of arrival and non-linear least square method for the localization of an RF transmitter inside the human body was presented. A formulation for the distance estimate between the in-body transmitter and an on-body receiver was derived based on the phase difference of the signal from the same burst at the receiver. A linear least square method was used for the estimation of the initial coordinates of the transmitter. This initial estimate was used as an input for the non-linear least square method for more accurate position estimation. The proposed method was applied on noise-free FDTD simulated data obtained through simulation with a simple homogeneous phantom, and a more realistic heterogeneous phantom, respectively. The error distance of the position estimate was within 1 cm after the implementation of the nonlinear least square method in the 2D case for the homogeneous and the heterogeneous phantom. The proposed algorithm was extended to a 3D case for the homogeneous cylinder case again giving the error distance within 1 cm. Hence, the presented algorithm is a possible candidate for localization of wireless capsule endoscopy, as long as the signal to noise ratio is high enough. Investigation directions for future work on the dependency of position estimate on number of receivers, polarization, and proper estimation of electric properties of the tissues were discussed.

7. REFERENCES

[1] G. Ciuti, A. Menciassi, P. Dario, "Capsule Endoscopy: From Current Achievements to Open Challenges", *IEEE Reviews in Biomed. Engg.*, vol. 4, pp. 59-72, 2011

[2] T.D. Than, G. Alici, H. Zhou, Weihua Li, "A Review of Localization Systems for Robotic Endoscopic Capsules", *IEEE Transactions on Biomed. Engg*, vol. 59, no. 9, pp. 2387-2399, Sept. 2012

[3] D. Manteuffel, M. Grimm, "Localization of a functional capsule for wireless neuro-endoscopy", in *Proc. Biomed. Wireless Tech., Net., Sensing Sys.*, BioWireleSS, pp. 61-64, Jan. 2012

[4] K. Arshak , F. Adepoju and D. Waldron, "A review and adaptation of methods of object tracking to telemetry capsules", *Int. J. Intell. Comput. Med. Sci. Image Process*, vol. 1, pp. 35-46, 2007

[5] K.Pahlavan, G. Bao, Y. Ye, S. Makarov, et. al., "RF Localization for Wireless Video Capsule Endoscopy", *Int. Journal Wireless Inf. Net.*, Vol. 19, pp. 326-340, 2012

[6] K. Arshak and F. Adepoju, "Adaptive linearized methods for tracking a moving telemetry capsule", in *Proc. IEEE Int. Symp. Ind. Electron*, pp. 2703-2708, 2007

[7] D. Fischer , R. Shreiber , G. Meron , M. Frisch , H. Jacob , A. Glukhovsky and A. Engel, "Localization of the wireless capsule endoscope in its passage through the GI tract", *Gastrointestinal Endoscopy*, vol. 53, AB126, 2001

[8] T. Shah , S. M. Aziz and T. Vaithianathan, "Development of a tracking algorithm for an in-vivo RF capsule prototype", in *Proc. Int. Conf. Electr. Comput. Eng.*, pp. 173-176, 2006

[9] W. Lujia , H. Chao , T. Longqiang , L. Mao and M. Q. H. Meng, "A novel radio propagation radiation model for location of the capsule in GI tract", *Proc. IEEE Int. Conf. Rob. Biomimetics*, pp. 2332-2337, 2009

[10] W. Lujia , L. Li , H. Chao and M. Q. H. Meng, "A novel RF-based propagation model with tissue absorption for location of the GI tract", *Proc. Annu. Int. Conf. IEEE Eng. Med. Biol. Soc.*, pp. 654-657, 2010

[11] K. Arshak and F. Adepoju, "A Method for Estimating the Geometric Position of a Wireless Telemetry Capsule in Real-Time", in *Proc. of European Conf. on Wireless Tech.*, pp. 193,196, Oct. 2007

[12] W. Yi, F. Ruijun, Y. Yunxing, U. Khan and K. Pahlavan, "Performance bounds for RF positioning of

endoscopy camera capsules", *Proc. IEEE Top. Conf. Biomed. Wireless Technol.*, Netw., Sens. Syst., pp. 71-74, 2011

[13] H. Jinlong, et. al., "Design and implementation of a high resolution localization system for in-vivo capsule endoscopy", in *Proc. 8th Int. conf. Dependable Auton. Secure Comput.*, pp. 209-214, 2009

[14] Z. Le, Z. Yongxin, M. Tingting, H. Jinlong and H. Hao, "Design of 3D positioning algorithm based on RFID receiver array for in vivo micro-robot", in *Proc. 8th IEEE Int. Conf. Dependable, Auton. Secure Comput.*, pp. 749-753, 2009

[15] L. Zhang, Y. Zhu, T. Mo, J. Hou and G. Rong, "Design and implementation of 3D positioning algorithms based on RF signal radiation patterns for in vivo micro-robot", in *Proc. Int. Conf. Body Sens. Netw.*, pp. 255-260, 2010

[16] C. Hekimian-Williams, B. Grant, L. Xiuwen , Z. Zhenghao and P. Kumar, "Accurate localization of RFID tags using phase difference",in *Proc. IEEE Int. Conf. Radio Freq. Identif.*, pp. 89-96, 2010

[17] A. Wille, M. Broll and S. Winter, "Phase difference based RFID navigation for medical applications", in *Proc. IEEE Int. Conf. Radio Freq. Identif.*, pp. 98-105, 2011

[18] M. Pourhomayoun, M. Fowler, Zhanpeng Jin, "A novel method for medical implant in-body localization", in *Proc. Annual Int. Conf. IEEE Eng. Med. Bio. Soc.*, EMBC, pp. 5757-5760, Sept. 2012

[19] W. Murphy and W. Hereman, "Determination of a position in three dimensions using trilateration and approximate distances", *Technical Report MCS-95-07*, Department of Mathematical and Computer Sciences, Colorado School of Mines, Golden, Colorado, 1995

[20] [Online]. Available: http://www.givenimaging.com/

[21] N.N. Rao, *Elements of Engineering Electtromagnetics*, 5th Edition, Prentice-Hall, 2000

[22] A. Christ et al., "The virtual family development of anatomical CAD models of two adults and two children for dosimetric simulations", *Phy. Med. Bio.*, vol. 55, no. 2, pp. N23-N38, Jan. 2010

[23] [Online]. Available: http://www.speag.com/products/semcad/solutions/